

High-performance bimetallic Ni-Mn Phosphate hybridized with 3-D graphene foam for novel hybrid supercapacitors

Abdulmajid A. Mirghni, Kabir O. Oyedotun, Oladepo Fasakin, Badr A. Mahmoud, Delvina Japhet
Tarimo and Ncholu Manyala*

Department of Physics, Institute of Applied Materials, SARChI Chair in Carbon Technology and Materials, University of Pretoria, Pretoria 0028, South Africa.

*Corresponding author's email: ncholu.manyala@up.ac.za, Tel.: + (27)12 420 3549

Supporting Information

Figure S1(a) shows XRD pattern of a characteristic as-prepared GF specifying diffraction peaks at about $2\theta = 27^\circ$ and 55° equivalent to the (002) and (004) reflections of hexagonal graphite respectively. Since Raman spectroscopy is very sensitive to stretching vibrations in molecules it can be used to identify different phases at the molecular level. Figure S1(b) represents Raman spectra of the as-prepared graphene foam. The figure shows a typical Raman spectrum of graphene which depicts G-mode (carbon-carbon vibration mode) at 1570 cm^{-1} and 2D-mode (originating from the double resonance process) at 2710 cm^{-1}

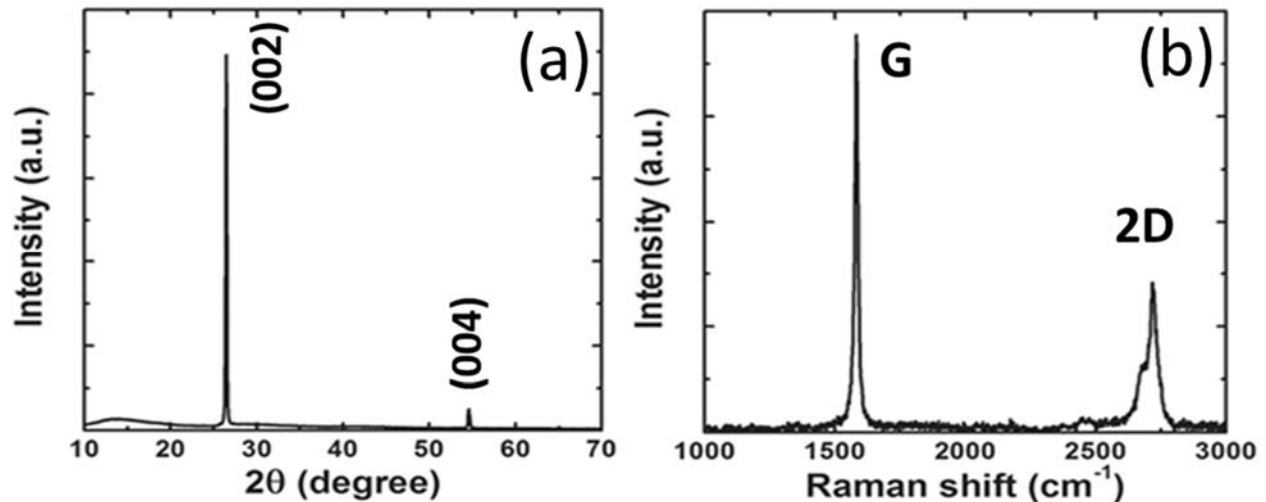


Figure S1. (a) XRD pattern and (b) Raman spectra of GF prepared by CVD system

Figure S2(a) represent SEM micrograph of the as-prepared graphene foam (GF) at 300 nm. The GF shows a typical sheet-like morphology of CVD graphene suggesting a high quality graphene foam. Figure S2(b) shows TEM micrograph of the GF which also confirms a typical sheet-like surface of GF. To get the thickness (number of layers) of the graphene foam (GF) used to make a composite, the GF sheet was investigated using HRTEM and the HRTEM micrograph of a GF sheet is shown in Fig. S2(c) along with the corresponding selected area electron diffraction (SAED) pattern (Fig. S2(d)). The HRTEM micrograph of GF displays folded area showing fringes (2-folds) corresponding to two layers of graphene which has a distinctively selected area electron diffraction pattern (SAED) of a graphene, as shown in Fig. S2(d). This suggests that a GF used in this work is a few-layered graphene foam and it is high- quality graphene.

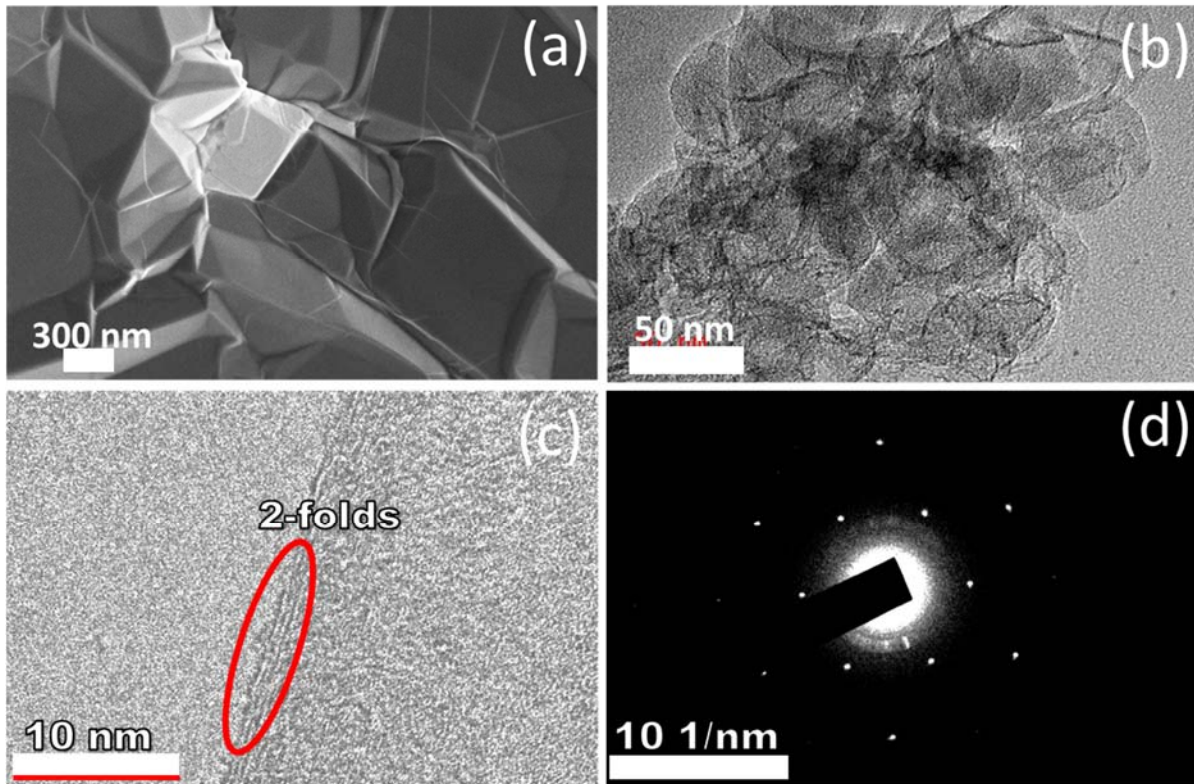


Figure S2. (a & b) SEM and TEM micrographs of graphene foam (GF) before being crushed into powder and sonicated, (c) HRTEM image of the GF at high magnification and (d) the corresponding SAED image

Figure S3 shows the CV curves of pristine $\text{NiMn}(\text{PO}_4)_2$, $\text{NiMn}(\text{PO}_4)_2/20$ mg GF, $\text{NiMn}(\text{PO}_4)_2/40$ mg GF, $\text{NiMn}(\text{PO}_4)_2/60$ mg GF, $\text{NiMn}(\text{PO}_4)_2/80$ mg GF and $\text{NiMn}(\text{PO}_4)_2/100$ mg GF composites at a scan rate of 20 mV s^{-1} in a potential window range of 0.0–0.45 V. In this figure, it can be observed that the addition of 20 mg GF to the pristine $\text{NiMn}(\text{PO}_4)_2$ could slightly improve the current response of the electrode material. However, $\text{NiMn}(\text{PO}_4)_2/80$ mg GF composite shows the highest

current response suggesting a high specific capacity according to equation (1) as reported in the main manuscript, and this could be attributed to the presence of an optimum amount of GF which effectively synergize with $\text{NiMn}(\text{PO}_4)_2$ and improves its electrical conductivity. $\text{NiMn}(\text{PO}_4)_2/100$ mg GF composite shows a decrease in current response compared to $\text{NiMn}(\text{PO}_4)_2/80$ mg GF composite and that could be due to the overlying of GF on $\text{NiMn}(\text{PO}_4)_2$ which negatively affects the synergy between the $\text{NiMn}(\text{PO}_4)_2$ and the GF.

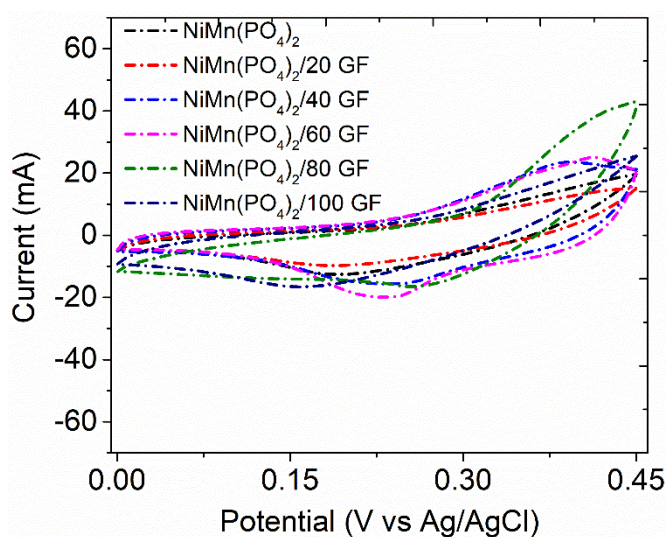


Figure S3. CV curves of the pristine $\text{NiMn}(\text{PO}_4)_2$ and $\text{NiMn}(\text{PO}_4)_2/\text{GF}$ composites at different GF mass loading measured at scan rate of 20 mV s^{-1}